JOC Article

Polycyclic Benzenoids: Why Kinked is More Stable than Straight

Jordi Poater,[†] Ruud Visser,[†] Miquel Solà,*[,‡] and F. Matthias Bickelhaupt*[,†]

Afdeling Theoretische Chemie, Scheikundig Laboratorium der Vrije Universiteit, De Boelelaan 1083, NL-1081 HV Amsterdam, The Netherlands, and Institut de Química Computacional and Departament de Química, Universitat de Girona, Campus Montilivi, E-17071 Girona, Catalonia, Spain

miquel.sola@udg.es; fm.bickelhaupt@few.vu.nl

Received August 7, 2006

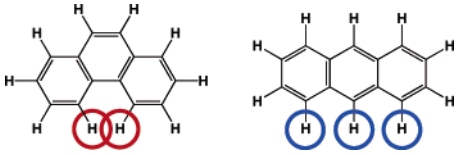

The enhanced stability of bent or kinked polycyclic benzenoids over linear ones is well established, phenanthrene and anthracene being archetypal representatives. The question why kinked is more stable than linear is, however, still a matter of discussion. Recently, it has been proposed that H−H bonding interactions between the two hydrogen atoms in the bay region of phenanthrene are responsible for the larger stability of this molecule as compared to anthracene. This conclusion conflicts with the vast body of evidence for nonbonded steric repulsion between these hydrogen atoms. In this work, we provide new, complementary evidence for the repulsive character of the H−H interactions in phenanthrene's bay region. We have traced the origin of phenanthrene's enhanced stability to the more efficient bonding in the π-electron system using, among others, a quantitative energy decomposition analysis of the bonding between the two constituting 2-methtriyl-phenyl fragments in both phenanthrene and anthracene (i.e., $C_{14}H_{10} = C_6H_4^{\bullet}-CH^{\bullet\bullet} + C_6H_4^{\bullet}-CH^{\bullet\bullet}$). The scope of our study is extended to polycyclic benzenoids by analyzing also hexacene and various bent isomers of the latter. Our results once more falsify one of the core concepts of the theory of atoms-in-molecules (AIM), namely, that the presence of bond paths and the presence of bond critical points (they exist indeed between the two bay H atoms in phenanthrene) are sufficient indicators for a stabilizing interaction. Instead, our results confirm that these AIM parameters merely diagnose the proximity or contact between charge distributions, be this contact stabilizing or destabilizing.

1. Introduction

The $C_{14}H_{10}$ isomers anthracene (**1**) and phenanthrene (**2**) are the simplest representatives of the class of linear and bent catacondensed polycyclic benzenoids, respectively.

The introduction of a kink in the linear benzenoid structure, that is, going from **1** to **2**, has important consequences for stability, electronic, and magnetic properties.[1−4] The photoelectron spectra, for example, show that the first ionization potential

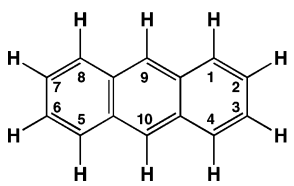

1

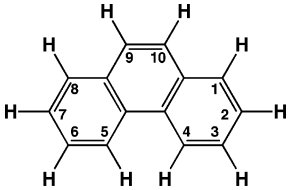

2

of **2** is 0.4 eV higher than that of **1**.[2,4] On the other hand, theoretical calculations indicate a larger HOMO−LUMO gap for **2**,[3] which is corroborated by the experimentally observed blue shift of the $S_1 \rightarrow S_0$ transition when going from **1** to **2**.[2] Furthermore, electronic ring currents in **1** are mainly localized in the central hexagon whereas in **2** they are strongest in the terminal hexagons[5,6] which translates into different magnetizability values and nuclear magnetic shielding tensors.[6]

* To whom correspondence should be addressed. Fax: +31-20-59-87629 (F.M.B.); +34-97-24-18356 (M.S.).
[†] Scheikundig Laboratorium der Vrije Universiteit.
[‡] Universitat de Girona.

(1) *NIST Chemistry WebBook;* NIST Standard Reference Database Number 69, June 2005 release. http://webbook.nist.gov/chemistry. Coleman, D. J.; Pilcher, G. *Trans. Faraday Soc.* **1966**, *62*, 821.
(2) Dabestani, R.; Ivanov, I. N. *Photochem. Photobiol.* **1999**, *70*, 10.
(3) Kato, T.; Yoshizawa, K.; Hirao, K. *J. Chem. Phys.* **2002**, *116*, 3420.
(4) Boschi, R.; Clar, E.; Schmidt, W. *J. Chem. Phys.* **1974**, *60*, 4406.

10.1021/jo061637p CCC: $37.00
Published on Web 01/17/2007

Possibly the most striking effect of introducing a kink, from **1** to **2**, is the enhanced stability of the bent isomer: it is well documented by various experimental[1,2,7] and theoretical studies[3,8−12] that phenanthrene (**2**) is 4−8 kcal/mol more stable than anthracene (**1**). This was rationalized already in 1933 by Pauling and Sherman[13] in terms of more efficient resonance in the π-electron system and, later on, through Clar's model of aromaticity[10,14] in terms of the larger number of "aromatic π sextets" in **2** (namely, 2 sextets) than in **1** (namely, 1 sextet). Indeed, there is now a general consensus about the higher aromaticity of phenanthrene as compared to anthracene.[3,8,12,15]

The above classical picture of phenanthrene's enhanced stability (and that of other bent polycyclic benzenoids) deriving from better π bonding has recently been questioned by Matta, Hernández-Trujillo, Tang, and Bader (MHTB)[11] on the basis of atoms-in-molecules (AIM) analyses.[16,17] MHTB claim to have evidence for stabilizing hydrogen−hydrogen bonding interactions (as opposed to nonbonded steric repulsion) between the two hydrogen atoms in the bay region of phenanthrene (H4 and H5, see **2**), in the form of the existence of a bond path between the two H nuclei and the corresponding bond critical point. In addition, according to the AIM calculations, hydrogen atoms taking place in the supposed H−H bonding are about 5 kcal mol^{-1} stabilized in phenanthrene with respect to "noninteracting" hydrogen atoms in the linear isomer. This was interpreted by MHTB as a stabilization of the overall molecular energy by 10 kcal/mol because of H−H bonding and the origin of the increased stability of phenanthrene relative to anthracene and, more generally, of [*n*]phenacenes as compared to their isomeric [*n*]acenes.[11]

However, there is an increasing body of evidence that the physical interpretation of AIM concepts, such as bond paths and atomic stabilization energies, is unclear. In particular, the hypothesis in AIM theory that the presence of a bond path is a necessary and, importantly, also a sufficient condition for the existence of a bonding interaction has been repeatedly shown unlikely[18−20] or even erroneous.[20,21] In an excellent and comprehensive review about bonding in organic crystals, Dunitz and Gavezzotti[22] note in connection with AIM's supposed 10 kcal/mol H−H bonding in phenanthrene the following:

The concept of "hydrogen−hydrogen bonding" is offered as an explanation for the relative thermodynamic stability of phenanthrene over anthracene and of chrysene over tetracene. This is clearly an unorthodox and challenging proposal because chemists have their own way of deciding which atoms are bonded to which in a molecule, and it clashes seriously with the chemist's picture. Besides, there are alternative explanations of the relative stability of phenanthrene and anthracene, based on qualitative comparison of the resonance stabilization of the two molecules.

It is, however, fair to add that Dunitz and Gavezzotti[22] do not dismiss AIM theory. Furthermore, Haaland et al.[21] have shown that helium's AIM atomic energy is dramatically (more than 300 kcal/mol) stabilized when it is brought from the gas phase into adamantane in the inclusion complex He@adamantane, despite the strongly antibonding He−C^t interactions taking place in the complex which is destabilized by about 150 kcal/mol relative to separate He + adamantane. The origin of the problem is that the interpretation in AIM theory of its core concepts is flawed: bond paths and bond critical points do not indicate bonding, they merely indicate proximity or contact between the two atomic charge densities involved. This has been repeatedly pointed out by others and by us[19−21,23−26] (see, however, the rebuttal in ref 27).

In the present study, we address the question why phenanthrene (**2**) is more stable than anthracene (**1**). Is the classical model of better π bonding in **2** valid? If so, why exactly is π bonding more stabilizing in **2** than in **1**? Or, is phenanthrene (**2**) more stable because of H−H bonding between the bay hydrogen atoms, as postulated in the AIM study of MHTB? To answer these questions, we have carried out an extensive analysis of the bonding in anthracene and phenanthrene using density functional theory (DFT)[28] at BLYP/TZ2P.[29,30] We analyze the bonding mechanism between the two 2-methtriylphenyl (**A**) fragments that make up both phenanthrene and

(5) Steiner, E.; Fowler, P. W. *Int. J. Quantum Chem.* **1996**, *60*, 609. Anusooya, Y.; Chakrabarti, A.; Pati, S. K.; Ramasesha, S. *Int. J. Quantum Chem.* **1998**, *70*, 503. Lazzeretti, P. In *Progress in Nuclear Magnetic Resonance Spectroscopy;* Emsley, J. W., Feeney, J., Sutcliffe, L. H., Eds.; Elsevier: Amsterdam, 2000; Vol. 36, p 1. Steiner, E.; Fowler, P. W.; Havenith, R. W. A. *J. Phys. Chem. A* **2002**, *106*, 7048.

(6) Ligabue, A.; Pincelli, U.; Lazzeretti, P.; Zanasi, R. *J. Am. Chem. Soc.* **1999**, *121*, 5513.

(7) Biermann, D.; Schmidt, W. *J. Am. Chem. Soc.* **1980**, *102*, 3163. Biermann, D.; Schmidt, W. *J. Am. Chem. Soc.* **1980**, *102*, 3173.

(8) Balaban, A. T. *Pure Appl. Chem.* **1980**, *52*, 1409.

(9) Behrens, S.; Köster, A. M.; Jug, K. *J. Org. Chem.* **1994**, *59*, 2546. Moyano, A.; Paniagua, J. C. *J. Org. Chem.* **1991**, *56*, 1858. Moyano, A.; Paniagua, J. C. *Trends Org. Chem.* **1993**, *4*, 697.

(10) Randić, M. *Chem. Rev. (Washington, D. C.)* **2003**, *103*, 3449.

(11) Matta, C. F.; Hernández-Trujillo, J.; Tang, T.-H.; Bader, R. F. W. *Chem.*−Eur. J. **2003**, *9*, 1940.

(12) Fukui, K. *Science* **1982**, *218*, 747.

(13) Pauling, L.; Sherman, J. *J. Chem. Phys.* **1933**, *1*, 606.

(14) Clar, E. *The Aromatic Sextet;* Wiley: New York, 1972. Portella, G.; Poater, J.; Solà, M. *J. Phys. Org. Chem.* **2005**, *18*, 785.

(15) Cyrański, M. K.; Stepién, B. T.; Krygowski, T. M. *Tetrahedron* **2000**, *56*, 9663. Portella, G.; Poater, J.; Bofill, J. M.; Alemany, P.; Solà, M. *J. Org. Chem.* **2005**, *70*, 2509; Erratum, ibid, **2005**, *70*, 4560. Hemelsoet, K.; Van Speybroeck, V.; Marin, G. B.; De Proft, F.; Geerlings, P.; Waroquier, M. *J. Phys. Chem. A* **2004**, *108*, 7281.

(16) Bader, R. F. W. *Acc. Chem. Res.* **1985**, *18*, 9. Bader, R. F. W. *Chem. Rev.* **1991**, *91*, 893. Bader, R. F. W. *Can. J. Chem.* **1998**, *76*, 973. Bader, R. F. W. *J. Phys. Chem. A* **1998**, *102*, 7314. Bader, R. F. W.; Matta, C. F.; Cortés-Guzmán, F. *Organometallics* **2004**, *23*, 6253.

(17) Bader, R. F. W. *Atoms in Molecules: A Quantum Theory*; Clarendon: Oxford, U.K., 1990.

(18) Martín Pendás, A.; Costales, A.; Luaña, V. *Phys. Rev. B* **1997**, *55*, 4275. Abramov, Y. A. *J. Phys. Chem. A* **1997**, *101*, 5725. Tsirelson, V.; Abramov, Y. A.; Zavodnik, V.; Stash, A.; Belokoneva, E.; Stahn, J.; Pietsch, U.; Feil, D. *Struct. Chem.* **1998**, *9*, 249. Tsirelson, V. G.; Avilov, A. S.; Lepeshov, G. G.; Kulygin, A. K.; Pietsch, U.; Spence, J. C. H. *J. Phys. Chem. B* **2001**, *105*, 5068. Cioslowski, J.; Edgington, L.; Stefanov, B. B. *J. Am. Chem. Soc.* **1995**, *117*, 10381. Farrugia, L. J.; Evans, C.; Tegel, M. *J. Phys. Chem. A* **2006**, *110*, 7952.

(19) Cioslowski, J.; Mixon, S. T. *J. Am. Chem. Soc.* **1992**, *114*, 4382.

(20) Cioslowski, J.; Mixon, S. T. *Can. J. Chem.* **1992**, *70*, 443.

(21) Haaland, A.; Shorokhov, D. J.; Tverdova, N. V. *Chem.*−Eur. J. **2004**, *10*, 4416.

(22) Dunitz, J. D.; Gavezzotti, A. *Angew. Chem.* **2005**, *117*, 1796; *Angew. Chem., Int. Ed.* **2005**, *44*, 1766.

(23) Poater, J.; Solà, M.; Bickelhaupt, F. M. *Chem.*−Eur. J. **2006**, *12*, 2889.

(24) Poater, J.; Solà, M.; Bickelhaupt, F. M. *Chem.*−Eur. J. **2006**, *12*, 2902.

(25) Frenking, G. *Angew. Chem.* **2003**, *115*, 152*; Angew. Chem., Int. Ed.* **2003**, *42*, 152. Feinberg, M. J.; Ruedenberg, K. *J. Chem. Phys.* **1971**, *54*, 1495.

(26) Frenking, G.; Esterhuysen, C.; Kovacs, A. *Chem.*−Eur. J. **2006**, *12*, 7573.

(27) Bader, R. F. W. *Chem.*−Eur. J. **2006**, *12*, 2896.

(28) Parr, R. G.; Yang, W. *Density-functional theory of atoms and molecules;* Oxford Univesity Press: New York, 1989. Kohn, W.; Sham, L. *J. Phys. Rev. A* **1965**, *140*, 1133.

(29) Becke, A. D. *Phys. Rev. A* **1988**, *38*, 3098. Lee, C.; Yang, W.; Parr, R. G. *Phys. Rev. B* **1988**, *37*, 785.

anthracene (i.e., $C_{14}H_{10} = C_6H_4^{\bullet}-CH^{\bullet\bullet} + C_6H_4^{\bullet}-CH^{\bullet\bullet}$) in the conceptual framework of the molecular orbital (MO) model that is contained in Kohn−Sham DFT and we carry out a quantitative decomposition of the bond energy into electrostatic attraction, Pauli repulsion (which is responsible for any steric repulsion), and bonding orbital interactions.[31,32]

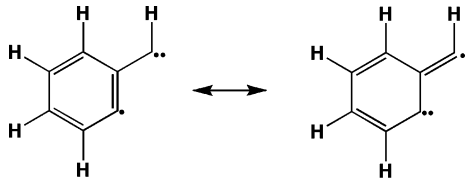

A

Our MO analyses reveal better π bonding in phenanthrene and simultaneously H−H steric repulsion, not H−H bonding, between the bay hydrogen atoms. Inspired by this outcome, we have designed several numerical experiments used to study derivatives of anthracene and phenanthrene in which (the bay) hydrogen atoms have been removed. This enables us to verify, independently of our or any other electronic structure model, if the bay hydrogen atoms in phenanthrene provide a stabilizing contribution, as hypothesized by MHTB, or if they cause repulsion and destabilization, as our analyses show. The validity of our conclusions for larger polycyclic benzenoids is explored using hexacene and various kinked isomers thereof. The scope of our findings extends, however, beyond the model systems studied here. They shed light on the status and interpretation of the very concepts of bond paths, bond critical points, and atomic energy in AIM theory. Here, we anticipate that our findings provide further evidence for fundamental flaws in the interpretation of topological parameters in AIM theory. In particular, they show once more[19−21,23−26] that the existence of a bond path with a bond critical point is not a sufficient condition for the presence of bonding interactions.

2. Methods

2.1. Computational Details. All calculations have been performed with the BLYP[29] functional and the TZ2P basis set using the Amsterdam Density Functional (ADF) program,[30] unless stated otherwise (vide infra). The TZ2P basis set is a large uncontracted set of Slater-type orbitals (STOs), containing diffuse functions, which is of triple-ζ quality and has been augmented with two sets of polarization functions: 2p and 3d on hydrogen and 3d and 4f on carbon. The core shell of carbon (1s) was treated by the frozen-core approximation.[30] An auxiliary set of s, p, d, f, and g STOs was used to fit the molecular density and to represent the Coulomb and exchange potentials accurately in each SCF cycle.[30] Relativistic effects were accounted for using the zeroth-order regular approximation (ZORA).[33] All stationary points have been confirmed to be equilibrium structures through vibrational analyses (i.e., zero imaginary frequencies). The AIM analyses[17,34] in this study have, for technical reasons, been carried out with the Gaussian 03[35] suite of programs at the BLYP/6-311G(df,pd) level in combination with the AIMPAC program.[34,35]

2.2. Bond Analysis. To obtain a deeper insight into the origin of the higher stability of phenanthrene, an energy decomposition analysis has been carried out.[31,32,36−38] In this analysis, the total binding energy ΔE associated with forming the anthracene or phenanthrene molecule from two identical 2-methtriyl-phenyl (**A**) triradicals with opposite spin:

$$\mathbf{A}^{\alpha\alpha\alpha} + \mathbf{A}^{\beta\beta\beta} \rightarrow \mathbf{1} \text{ or } \mathbf{2}\text{: } \Delta E \tag{1}$$

is made up of two major components (eq 2):

$$\Delta E = \Delta E_{\text{prep}} + \Delta E_{\text{int}} \tag{2}$$

In this formula, the preparation energy ΔE_{prep} is the amount of energy required to deform two individual (isolated) triradicals from their equilibrium structure to the geometry that they acquire in the overall molecule. The interaction energy ΔE_{int} corresponds to the actual energy change when these geometrically deformed triradicals are combined to form the anthracene or phenanthrene molecules. It is analyzed in the framework of the Kohn−Sham molecular orbital (MO) model using a quantitative decomposition of the bond into electrostatic interaction, Pauli repulsion (or exchange repulsion or overlap repulsion), and (attractive) orbital interactions (eq 3).[31]

$$\Delta E_{\text{int}} = \Delta V_{\text{elstat}} + \Delta E_{\text{Pauli}} + \Delta E_{\text{oi}} \tag{3}$$

The term ΔV_{elstat} corresponds to the classical electrostatic interaction between the unperturbed charge distributions $\rho_{\mathbf{A}}{}^{\alpha\alpha\alpha} + \rho_{\mathbf{A}}{}^{\beta\beta\beta}$ of the prepared (i.e., deformed) triradicals (vide infra for definition of the fragments) that adopt their positions in the overall molecule and is usually attractive. The Pauli repulsion term, ΔE_{Pauli}, comprises the destabilizing interactions between occupied orbitals and is responsible for the steric repulsion. This repulsion is caused by the fact that two electrons with the same spin cannot occupy the same region in space. It arises as the energy change associated with the transition from the superposition of the unperturbed electron densities $\rho_{\mathbf{A}}{}^{\alpha\alpha\alpha}$

(30) Baerends, E. J.; Ellis, D. E.; Ros, P. *Chem. Phys.* **1973**, *2*, 41. Fonseca Guerra, C.; Snijders, J. G.; te Velde, G.; Baerends, E. J. *Theor. Chem. Acc.* **1998**, *99*, 391. te Velde, G.; Bickelhaupt, F. M.; Baerends, E. J.; Fonseca Guerra, C.; van Gisbergen, S. J. A.; Snijders, J. G.; Ziegler, T. *J. Comput. Chem.* **2001**, *22*, 931.

(31) Bickelhaupt, F. M.; Baerends, E. J. In *Reviews in Computational Chemistry*; Lipkowitz, K. B., Boyd, D. B., Eds.; Wiley-VCH: New York, 2000; Vol. 15, p 1. Kovacs, A.; Esterhuysen, C.; Frenking, G. *Chem.−Eur. J.* **2005**, *11*, 1813.

(32) Bickelhaupt, F. M.; Nibbering, N. M. M.; van Wezenbeek, E. M.; Baerends, E. J. *J. Phys. Chem.* **1992**, *96*, 4864.

(33) van Lenthe, E.; Baerends, E. J. *J. Chem. Phys.* **1993**, *99*, 4597. van Lenthe, E.; Baerends, E. J.; Snijders, J. G. *J. Chem. Phys.* **1994**, *101*, 9783. van Lenthe, E.; Ehlers, A. E.; Baerends, E. J. *J. Chem. Phys.* **1999**, *110*, 8943. van Lenthe, E.; Snijders, J. G.; Baerends, E. J. *J. Chem. Phys.* **1996**, *105*, 6505. van Lenthe, E.; van Leeuwen, R.; Baerends, E. J.; Snijders, J. G. *Int. J. Quantum Chem.* **1996**, *57*, 281.

(34) Biegler-König, F. W.; Bader, R. F. W.; Tang, T.-H. *J. Comput. Chem.* **1982**, *3*, 317 (http://www.chemistry.mcmaster.ca/aimpac/).

(35) Frisch, M. J.; Trucks, G. W.; Schlegel, H. B.; Scuseria, G. E.; Robb, M. A.; Cheeseman, J. R.; Montgomery, J. A., Jr.; Vreven, T.; Kudin, K. N.; Burant, J. C.; Millam, J. M.; Iyengar, S. S.; Tomasi, J.; Barone, V.; Mennucci, B.; Cossi, M.; Scalmani, G.; Rega, N.; Petersson, G. A.; Nakatsuji, H.; Hada, M.; Ehara, M.; Toyota, K.; Fukuda, R.; Hasegawa, J.; Ishida, M.; Nakajima, T.; Honda, Y.; Kitao, O.; Nakai, H.; Klene, M.; Li, X.; Knox, J. E.; Hratchian, H. P.; Cross, J. B.; Bakken, V.; Adamo, C.; Jaramillo, J.; Gomperts, R.; Stratmann, R. E.; Yazyev, O.; Austin, A. J.; Cammi, R.; Pomelli, C.; Ochterski, J. W.; Ayala, P. Y.; Morokuma, K.; Voth, G. A.; Salvador, P.; Dannenberg, J. J.; Zakrzewski, G.; Dapprich, S.; Daniels, A. D.; Strain, M. C.; Farkas, O.; Malick, D. K.; Rabuck, A. D.; Raghavachari, K.; Foresman, J. B.; Ortiz, J. V.; Cui, Q.; Baboul, A. G.; Clifford, S.; Cioslowski, J.; Stefanov, B. B.; Liu, G.; Liashenko, A.; Piskorz, P.; Komaromi, I.; Martin, R. L.; Fox, D. J.; Keith, T.; Al-Laham, M. A.; Peng, C. Y.; Nanayakkara, A.; Challacombe, M.; Gill, P. M. W.; Johnson, B.; Chen, W.; Wong, M. W.; Gonzalez, C.; Pople, J. A. *Gaussian 03*, Revison C.01 ed.; Gaussian, Inc.: Pittsburgh, PA, 2003.

(36) Kitaura, K.; Morokuma, K. *Int. J. Quantum Chem.* **1976**, *10*, 325. Ziegler, T.; Rauk, A. *Inorg. Chem.* **1979**, *18*, 1755.

(37) Morokuma, K. *Acc. Chem. Res.* **1977**, *10*, 294.

(38) Ziegler, T.; Rauk, A. *Theor. Chim. Acta* **1977**, *46*, 1. Ziegler, T.; Rauk, A. *Inorg. Chem.* **1979**, *18*, 1558.

TABLE 1. Analysis of the Bonding (in kcal/mol) between the Two 2-Methtriyl-phenyl Fragments (A) in Anthracene (1), Phenanthrene (2), and Deformed Phenanthrene Structures (2a and 2b)[a]

	1 A(1) + A(1)	**2** A(2) + A(2)	**2a** A(1) + A(1)	**2b** A(1) + A(1)
ΔE_{Pauli}	555.07	539.88 (−15.19)	545.09 (−9.98)	557.19 (2.12)
ΔV_{elstat}	−350.42	−342.11 (8.31)	−344.22 (6.20)	−350.94 (−0.52)
ΔE_{σ}	−400.75	−395.66 (5.09)	−397.03 (3.72)	−401.00 (−0.25)
ΔE_{π}	−83.02	−85.55 (−2.53)	−85.46 (−2.44)	−85.06 (−2.04)
ΔE_{int}	−279.12	−283.43 (−4.31)	−281.61 (−2.49)	−279.81 (−0.69)
ΔE_{prep}	8.08	8.15 (0.07)	8.08 (0.00)	8.08 (0.00)
ΔE	−271.04	−275.28 (−4.24)	−273.53 (−2.49)	−271.73 (−0.69)

[a] Computed at BLYP/TZ2P. **A(1)** and **A(2)** represent **A** in the geometry it adopts in **1** and **2**, respectively; **2a** is phenanthrene with frozen **A(1)** fragments but with C−C bond distances as in **2**; **2b** is phenanthrene with frozen **A(1)** fragments and with C−C bond distances as in **1**. Values in parentheses show the difference of the energy term with the corresponding one for **1** from **A(1)** + **A(1)**.

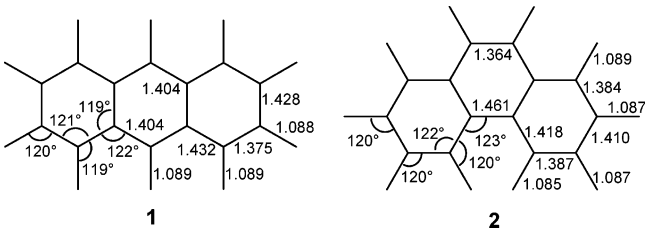

FIGURE 1. Equilibrium structures (in Å, deg) of anthracene (**1**) and phenanthrene (**2**) computed at BLYP/TZ2P.

$+ \rho_{\mathbf{A}}^{\beta\beta\beta}$ of the geometrically deformed but isolated triradicals to the wavefunction $\Psi^0 = N\hat{A}\,[\Psi_{\mathbf{A}}^{\alpha\alpha\alpha}\,\Psi_{\mathbf{A}}^{\beta\beta\beta}]$, that properly obeys the Pauli principle through explicit antisymmetrization ($\hat{A}$ operator) and renormalization (N constant) of the product of fragment wavefunctions (see ref 31 for an exhaustive discussion). The orbital interaction ΔE_{oi} in any MO model, and therefore also in Kohn−Sham theory, accounts for electron-pair bonding,[31] charge transfer (i.e., donor−acceptor interactions between occupied orbitals on one moiety with unoccupied orbitals of the other, including the HOMO−LUMO interactions), and polarization (empty−occupied orbital mixing on one fragment because of the presence of another fragment). In the bond-energy decomposition, open-shell fragments are treated with the spin-unrestricted formalism but, for technical (not fundamental) reasons, spin-polarization is not included. This error causes an electron-pair bond to become about a few kcal/mol too strong. To facilitate a straightforward comparison, the EDA results were scaled to match exactly the regular bond energies (the correction factor is consistently 0.935 in all model systems and does not, therefore, affect trends). Since the Kohn−Sham MO method of density-functional theory (DFT) in principle yields exact energies and, in practice, with the available density functionals for exchange and correlation, rather accurate energies, we have the special situation that a seemingly one-particle model (a MO method) in principle completely accounts for the bonding energy.[31,39]

The orbital interaction energy can be decomposed into the contributions from each irreducible representation Γ of the interacting system (eq 4) using the extended transition state (ETS) scheme developed by Ziegler and Rauk[38] (note that our approach differs in this respect from the Morokuma scheme,[37] which instead attempts a decomposition of the orbital interactions into polarization and charge transfer).

$$\Delta E_{\text{oi}} = \Sigma_{\Gamma}\,\Delta E_{\Gamma} \tag{4}$$

Results and Discussion

3.1. Anthracene and Phenanthrene. The results of our BLYP/TZ2P analyses are collected in Table 1 and Figure 1 (Cartesian coordinates for all stationary points can be found in the Supporting Information). In line with previous experimental[1,2,7] and theoretical studies,[8−11] we find that phenanthrene (**2**) is 4.24 kcal/mol more stable than anthracene.

To understand why the kinked isomer is more stable, we consider the formation of **1** and **2** from two identical 2-methtriyl-phenyl fragments **A**

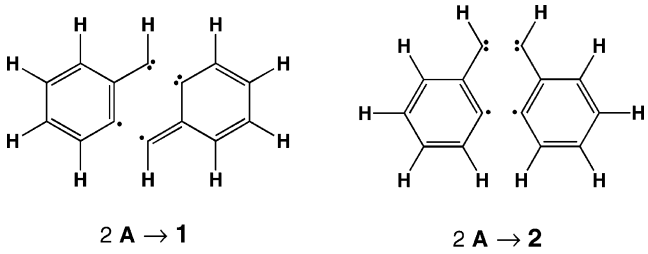

The formation of the overall tribenzenoid structures leads to small deformations within **A**. As can be seen in Figure 1, the C−C−H angle involving the H atom ortho to the arylic C atom formally carrying the radical electron in the isolated fragment widens slightly from 119° in **1** to 120° in **2**. We refer to the deformed 2-methtriyl-phenyl fragments as **A(1)** and **A(2)**, respectively. The most important geometrical difference between **1** and **2** occurs in the C−C bonds that connect the **A** fragments (see Figure 1). In **1**, they are equivalent and measure 1.404 Å (exp:[40] 1.403 Å). In **2**, the C−C bond in the sterically crowded bay is somewhat longer, 1.461 Å, and the other C−C bond is shorter, 1.364 Å (exp:[41] 1.468 and 1.341 Å).

Thus, formation of **1** and **2** from two **A** involves deforming the two triradical fragments after which they can form three electron-pair bonds: two in the σ-electron system and one in the π-electron system. As can be seen in Table 1, the overall bond energies ΔE from our analyses amount to −271.04 (**1**) and −275.28 (**2**) and yield correctly phenanthrene as the 4.24 kcal/mol more stable isomer. The enhanced stability of phenanthrene (**2**) does not originate from the deformation energies ΔE_{prep}: they are essentially equal for the two isomers with values of 8.08 and 8.15 kcal/mol for **1** and **2**, respectively (in fact, ΔE_{prep} is even slightly, i.e., 0.07 kcal/mol more destabilizing for **2**). It is the −4.31 kcal/mol more stabilizing interaction ΔE_{int} between the fragments **A** that causes the higher stability of phenanthrene (**2**) (see Table 1).

Further decomposition of ΔE_{int} seems, at first sight, to suggest reduced steric repulsion in phenanthrene (**2**) as the main reason

(39) Baerends, E. J.; Gritsenko, O. V. *J. Phys. Chem. A* **1997**, *101*, 5383.

(40) Brock, C. P.; Dunitz, J. D.; Hirshfeld, F. L. *Acta Crystallogr., Sect. B* **1991**, *47*, 789.

(41) Kay, M. I.; Okaya, Y.; Cox, D. E. *Acta Crystallogr., Sect. B* **1971**, *27*, 26.

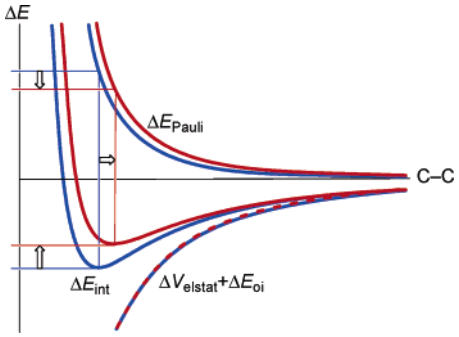

FIGURE 2. Schematic illustration of the interaction energy ($\Delta E_{int} = \Delta E_{Pauli} + \Delta V_{elstat} + \Delta E_{oi}$) as a function of the bond distance for two C−C bonds with equal bonding components ($\Delta V_{elstat} + \Delta E_{oi}$) but different steric repulsion (ΔE_{Pauli}). The C−C bond with ΔE_{Pauli} being more destabilizing at any given C−C distance (red curves) leads to a longer equilibrium distance in which ΔE_{Pauli} may adopt a smaller value than in the equilibrium structure of the sterically less demanding situation with its shorter bond distance (blue curves).

for the higher stability of this isomer: if one goes from **1** to **2**, the Pauli repulsion is lowered by −15.19 kcal/mol which is mainly due to reduced overlap between closed-shell orbitals on the **A** fragments with C−H-bonding character (not shown in Table 1). This observation is, however, misleading: direct comparison of **1** and **2** reflects not only the pure changes in bonding because of "flipping" the two **A** fragments from their relative orientation in anthracene (**1**) to that in phenanthrene (**2**). It also contains the effect of structural relaxation that is induced by the changes in intrinsic bonding but which also masks the latter. This structural relaxation consists of a change in the extent of deformation in **A**, which is minor and does not play a role here, as well as the more important changes in the length of the two C−C bonds that connect the **A** fragments (vide supra). Previously, we have shown that a situation with a larger Pauli repulsion, that is, with ΔE_{Pauli} being more destabilizing at any given C−C bond distance, leads to an equilibrium structure with a longer bond (and increased angles) in which eventually the Pauli repulsion term adopts a smaller value than in the equilibrium structure of the sterically less demanding situation with its shorter bond distance.[42] This is schematically illustrated in Figure 2. The more general lesson to be learned from this observation is that a one-shot analysis, that is, comparing two systems each only at their equilibrium geometry, is deceptive and may lead to erroneous conclusions.[42]

Thus, to reveal the intrinsic differences in **A**−**A** bonding between the two isomers, we have also analyzed a deformed phenanthrene structure **2b** that arises from anthracene (**1**) by only flipping the mutual orientation of the two 2-methtriyl-phenyl fragments **A(1)** to that of phenanthrene, while their geometry remains frozen and the distances of the two formed C−C bonds are kept fixed to the equilibrium distance of anthracene. This phenanthrene **2b** is still more stable than anthracene **1**, although the energy difference of −0.69 kcal/mol is smaller than the −4.24 kcal/mol that we find for the equilibrium structure of phenanthrene (**2**) (see Table 1). Importantly, however, any difference is now entirely due to the intrinsic differences in bonding associated with the two relative orientations between the **A(1)** fragments. The bond energy decomposition clearly shows that steric repulsion ΔE_{Pauli} becomes 2.12 kcal/mol more destabilizing if one goes from **1** to **2b** (see Table 1). The fact that **2b** is nevertheless more stable is caused by the other energy terms, that is, the changes in the electrostatic attraction ΔV_{elstat}, σ orbital interactions ΔE_σ, and π orbital interactions ΔE_π which contribute −0.52 (ΔV_{elstat}), −0.25 (ΔE_σ), and −2.04 kcal/mol (ΔE_π) (see Table 1). While none of these terms are unimportant, the predominant mechanism for enhancing the stability of phenanthrene **2b** is the π orbital interactions ΔE_π. This is important because if the H−H bonding postulated by MHTB on the basis of their AIM analyses would exist, then a stabilization in the σ orbital interactions ΔE_σ would have been the dominant driving force for the enhanced stability of phenanthrene **2b**.

The differences between **1** and **2b** can be better understood if we examine the three singly occupied molecular orbitals (SOMOs) of a 2-methtriyl-phenyl triradical **A(1)** which are depicted in Figure 3: these are the σ_A and σ_S orbitals in the σ-electron system and the π orbital in the π electron system. The former two are antisymmetric and symmetric regarding the sign of their large-amplitude lobes that build up bonding overlap in the $\sigma_A + \sigma_A$ and $\sigma_S + \sigma_S$ electron-pair bonding combinations in anthracene and phenanthrene. The $\pi + \pi$ combination is responsible for providing electron-pair bonding in the π-electron system. Note the textbook appearance of the π SOMO which is the nonbonding molecular orbital (NBMO) of our 2-methtriyl-phenyl fragment, an uneven alternating hydrocarbon (this π NBMO is probably better known from the one in benzyl which, in simple Hückel theory, is completely equivalent):[43] π has small coefficients on the ring and a large one on the exocyclic carbon atom. Best $\pi + \pi$ overlap (and π-electron-pair bonding) occurs if the high-amplitude lobe of one π can overlap with the high-amplitude lobe of the other π, that is, in phenanthrene.

Indeed, the $\pi + \pi$ overlap increases from 0.19 in anthracene (**1**) to 0.23 in phenanthrene **2b** (not shown in Table 1). The better π overlap in **2b** and the resulting stronger electron-pair bond in the π-electron system are illustrated in the schematic orbital interaction diagram of Figure 4 which is based on our quantitative analyses of the Kohn−Sham MO electronic structure. The $\pi + \pi$ bond in **2b** leads to stronger stabilization of the bonding combination than that in **1** (see blue levels in Figure 4). This increased stabilization of the $\pi + \pi$ bonding orbital in **2b**, which is the HOMO of the overall molecule, is in line with the experimental observation that phenanthrene has a larger HOMO−LUMO gap[2,3] and higher ionization potential.[2,4] In Figure 4, central panel, we also show the better $\pi + \pi$ overlap in **2b** in a more schematic manner. On the other hand, as pointed out above, there is more steric repulsion in **2b** between closed-shell fragment orbitals with "C−H" character. This is represented in Figure 4 with the red levels; a schematic representation of the increased repulsive overlap is shown in the lower panel. There are several closed-shell C−H orbitals in the fragments that overlap and cause Pauli repulsion, whereas for clarity, we show only one such interaction in Figure 4. Our results are consistent with complementary analyses by Fukui and Kato et al.[3,12] who compared the π orbital interactions (but not σ orbital interactions and steric repulsion) in the formation of anthracene and phenanthrene from naphthalene and butadiene fragments.

Finally, we allow **2b** to geometrically relax to its equilibrium structure. First, we lift only the constraint on the two C−C bonds

(42) Bickelhaupt, F. M.; Baerends, E. J. *Angew. Chem.* **2003**, *115*, 4315; *Angew. Chem., Int. Ed.* **2003**, *42*, 4183. Bickelhaupt, F. M.; DeKock, R. L.; Baerends, E. J. *J. Am. Chem. Soc.* **2002**, *124*, 1500.

(43) Murrell, J. N.; Kettle, S. F. A.; Tedder, J. M. *The Chemical Bond*, 2nd rev. ed.; John Wiley & Sons: New York, 1985.

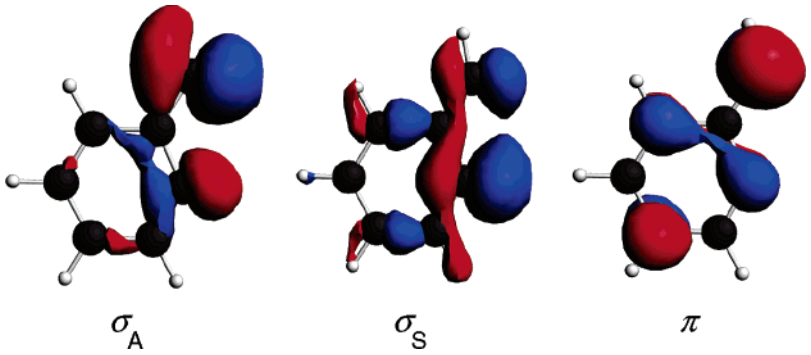

FIGURE 3. 3D-representation of the three SOMOs of a 2-methtriyl-phenyl fragment **A(1)**, obtained at BLYP/TZ2P (isosurface values are 0.045 and −0.045 au). Those of **A(2)** are essentially identical.

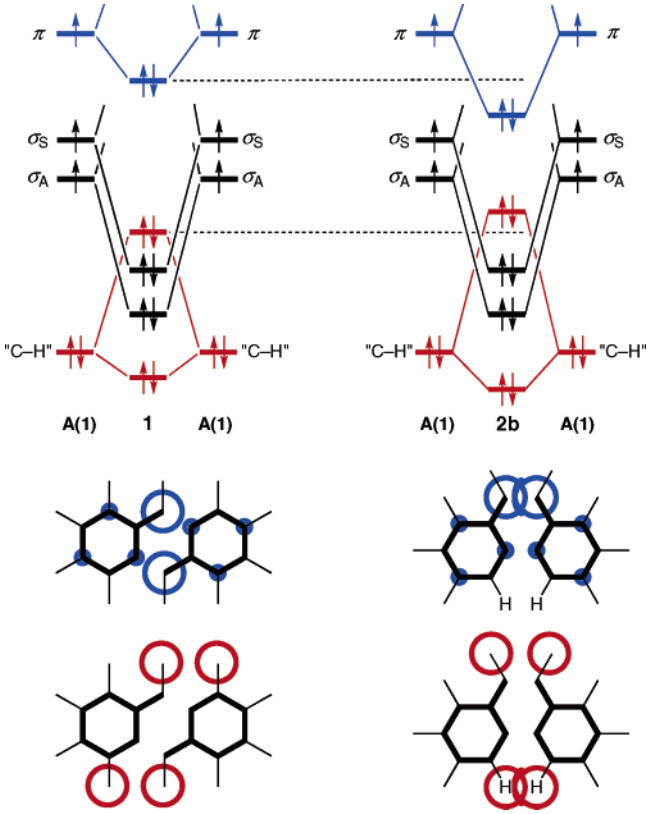

FIGURE 4. Upper panel: schematic diagram of the frontier-orbital interactions between identical 2-methtriyl-phenyl fragments **A(1)** in anthracene (**1**) and phenanthrene (**2b**) emerging from the Kohn−Sham MO analyses at BLYP/TZ2P. For clarity, only one of the Pauli-repulsive interactions between C−H closed-shell orbitals is shown. The dashed lines help in recognizing the main differences between **1** and **2b**. Central panel: bond overlap between the π SOMOs. Lower panel: repulsive overlap between closed-shell orbitals with C−H character.

connecting the otherwise still frozen **A(1)** fragments and allow these bonds to adopt the values in phenanthrene: this brings us to the phenanthrene structure **2a** (see Table 1). In line with the better $\pi + \pi$ bonding in the upper C−C bond (see Figure 4), this bond contracts from 1.404 (**2b**) to 1.364 Å (**2a**) whereas the lower one expands from 1.404 (**2b**) to 1.461 Å (**2a**). The lower C−C bond in the sterically crowded bay region also expands to reduce the repulsive H−H contact (see Figure 4). The bond energy decomposition reveals that this leads among others to a slight stabilization in π orbital interactions ΔE_π and a substantial reduction in Pauli repulsion. In a second step, the internal geometry of the fragments is allowed to relax from **A-(1)** to **A(2)** which brings us to the equilibrium structure of phenanthrene (**2**). The effects in this final step are less pronounced and more subtle. Note, however, the further reduction of the Pauli repulsion as the C−H bonds in the bay region bend away from each other (see Table 1 and Figure 1).

We have tried to isolate and directly compute the interaction between the bay hydrogen atoms in **2b** and **2**, that is, without any stabilizing or destabilizing contribution from other contacts (in particular, the C−C bonds). To achieve this, we analyze the interaction energy between two ethene fragments combined such that they have only one short contact, namely, an H−H contact of the same distance as that between the bay H atoms in phenanthrene (see structure **B**).

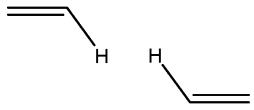

B

The two ethene fragments in **B** are of D_{2h} symmetry and their geometry corresponds to that of the phenanthrene bay fragment: C−C = 1.387 Å, C−H = 1.085 Å, and C−C−H = 118° just as C3−C4, C4−H4, and C3−C4−H4 in **2** (see Figure 1). When we place these two fragments as in **B** with a H−H separation of 2.021 Å, we found that **B** is less stable than the two separated fragments by 1.61 kcal/mol at BLYP/TZ2P. Yet, AIM analyses at BLYP/6-311G(df,pd) lead to an H−H bond critical point (bcp) in **B** and the combined AIM atomic stabilization energy for each of the two hydrogen atoms involved is −2.84 kcal/mol, suggesting again erroneously a H−H bond of −5.68 kcal/mol. The net destabilization of **B** by 1.61 kcal/mol is caused by a $\Delta E_{\text{Pauli}} = +3.42$ kcal/mol which is not compensated by the stabilizing energy terms $\Delta V_{\text{elstat}} = -0.94$, $\Delta E_\sigma = -0.84$, and $\Delta E_\pi = -0.03$ kcal/mol (ΔE_π), that is, hyperconjugation as measured by ΔE_σ is not stabilizing enough to surmount the Pauli repulsion and the whole interaction is clearly repulsive. This result is qualitatively not affected if one uses in **B** ethene molecules with their own equilibrium geometry instead of structures that are based on the phenanthrene bay fragment. Further support for steric H−H repulsion instead of bonding is provided, later on, by another numerical experiment that is also independent of any electronic structure model.

In conclusion, our analyses show that phenanthrene is more stable than anthracene because of better π bonding (in line with

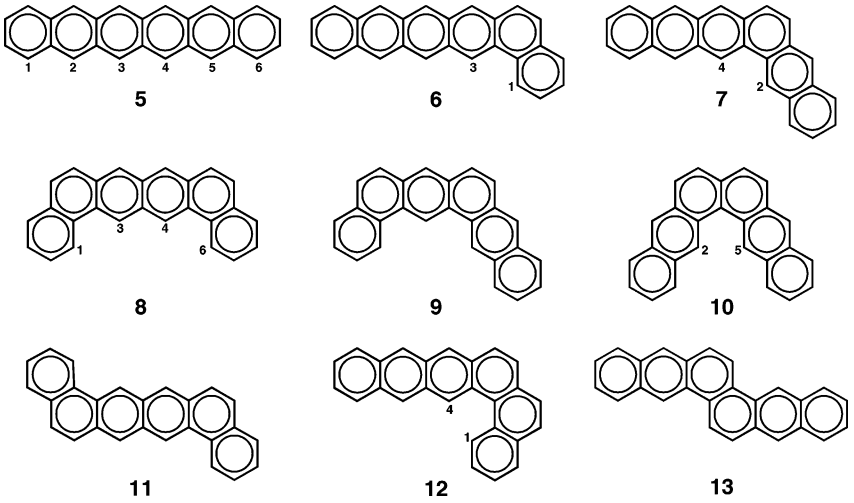

FIGURE 5. Linear (**5**) and kinked (**6**−**13**) hexacyclic benzenoids with position numbers used to designate selected di-dehydrogenated biradical species. See Table 2 for relative energies.

the classical picture) and despite an increased H−H steric repulsion between bay hydrogens (which falsifies MHTB's hypothesis of H−H bonding on the basis of AIM analyses). Interestingly, the intrinsic changes in bonding between the two **A** fragments in **1** and **2** are masked by the geometrical changes they induce. This illustrates once more that for a full understanding of chemical bonding, a "single-shot approach" (analysis of one geometry) does not often suffice. Instead, as pointed out before,[23,24,42] one must take such geometrical relaxation into account by following the electronic structure and bonding along the key points of the deformation mode.

3.2. Phenanthrene without Bay Hydrogen Atoms: A Numerical Experiment. The above results have inspired us to carry out a numerical experiment that complements the analyses. If there is steric H−H repulsion between the bay hydrogen atoms in phenanthrene, as our analyses show, then removing these hydrogen atoms should further increase the stability of the phenanthrene relative to the anthracene structure. On the other hand, if there would be H−H bonding (which is not what we find above but what MHTB[11] conclude from AIM analyses), then removing these hydrogen atoms should decrease the stability of the phenanthrene relative to the anthracene structure. Thus, in addition to **1** and **2**, we have computed the geometry and relative energies of the corresponding biradicals **3** and **4** in which H4 and H5 hydrogen atoms have been removed. The species **3** and **4** have been analyzed in their lowest-lying triplet states which correspond to their respective valence states in **1** and **2**.

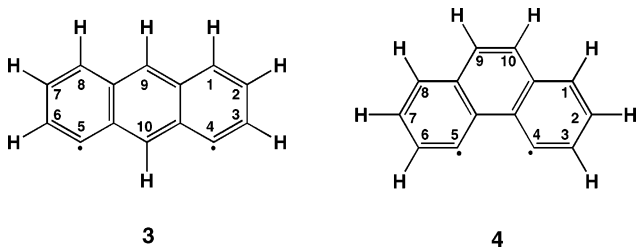

The numerical experiment confirms that there is H−H steric repulsion between phenanthrene's bay hydrogen atoms, no H−H bonding. In the parent molecules, phenanthrene (**2**) is 4.24 kcal/mol more stable than anthracene (**1**). Removing hydrogen atoms H4 and H5 makes the phenanthrene-derived species relatively more stable, not less: we find that **4** is 5.16 kcal/mol more stable than **3**. In line with this reduced H−H steric repulsion in the bay region of **4**, the lower C−C bond that is 1.461 Å in **2** contracts to 1.454 Å in **4** (see Supporting Information). Therefore, we can conclude again that phenanthrene is more stable than anthracene despite the presence of the bay hydrogens and really not because of them. This second falsification of MHTB's H−H bonding hypothesis is independent of any model of the electronic structure.

TABLE 2. Relative Energies ΔE_{rel} (in kcal/mol) and Geometry (Planar versus Nonplanar) of Hexacyclic Benzenoids and Selected Di-dehydrogenated Biradical Derivatives[a]

benzenoid	ΔE_{rel}[b]	geometry	benzenoid-2H	ΔE_{rel}	geometry
5	0.00	planar	1,3-[**5**−2H]	0.00[d]	planar
			2,4-[**5**−2H]	0.00[d]	planar
			3,4-[**5**−2H]	0.00[d]	planar
			1,4-[5−2H]	0.00[d]	planar
			2,5-[5−2H]	0.00[d]	planar
6	−8.75	planar	1,3-[6−2H]	−9.71	planar
7	−12.72	planar	2,4-[7−2H]	−13.78	planar
8	−16.25	planar	1,3-[8−2H]	−17.14	planar
			3,4-[8−2H]	−19.37	planar
9	−17.70	planar			
10	−8.34	nonplanar	2,5-[10−2H]	−13.10	planar
11	−16.27	planar			
12	−6.74	nonplanar	1,4-[12−2H]	−11.53	planar
13	−14.33	planar			

[a] Computed at BLYP/TZ2P. See Figure 5 for structures. Biradicals in triplet ground states. [b] All energies relative to **5**. [c] Energy of bent a,b-[**x**−nH] isomers relative to corresponding linear a,b-[**5**−nH] biradical (e.g., 1,3-[**6**−2H] relative to 1,3-[**5**−2H]). [d] The energies of all linear a,b-[**5**−2H] biradicals are equal within about half a kcal/mol.

3.3. Larger Polycyclic Benzenoids. In the previous sections, we have established that phenanthrene (**2**) is more stable than anthracene (**1**) because of more stabilizing π bonding and despite the destabilizing effect that the bay hydrogens have. Here, we extend our survey to larger polycyclic benzenoids using hexacene (**5**) and various (but not all) kinked and bifurcated isomers **6**−**13** (see Figure 5). We compare the energetics of these species as well as that of several biradical systems that derive from the parent benzenoids by removing two hydrogen atoms (see Table 2). These biradical systems are taken in their lowest-lying triplet state. Relative energies are calculated with

respect to the corresponding biradical structure of the linear acene **5**.

The results confirm the more general validity of our findings for **1** and **2**. Proceeding from the linear hexacene (**5**), the introduction of one kink (**6** and **7**) leads to a stabilization by some 9−13 kcal/mol (see Figure 5 and Table 2). This is not due to the H−H interaction in the bay region but despite this interaction which appears to be destabilizing. This is illustrated by the increase (not decrease!) of the relative stability of the kinked relative to the linear systems by an additional kcal/mol if the bay hydrogens are taken away leading to the corresponding biradicals in their lowest-lying triplet states. Thus, the kinked 1,3-[**6**−2H] and 2,4-[**7**−2H] are 10−14 kcal/mol more stable than the corresponding linear [**5**−2H] (see Table 2).

The trend continues if we introduce a second kink in the benzenoids (**8**−**13**) which leads to a more pronounced stabilization relative to **5**, namely, by 14−18 kcal/mol, as long as the kinks are not adjacent, that is, in **8**, **9**, **11**, and **13** (see Figure 5 and Table 2). Species **8** and **11** are *Z* and *E* isomers of the terminally double-kinked hexacyclic benzenoid and have essentially (within 0.02 kcal/mol) the same energy (see Table 2), in line with the fact that the two kinks are far apart from each other and experience the same local bay geometry at either terminus.

Interestingly, if the two kinks occur next to each other, that is, in **10** and **12**, H−H repulsion becomes particularly obvious (see Figure 5). In the merged bays of **10** and **12**, the positions of the two hydrogen atoms nearly coincide causing a severe deformation of the benzenoid which actually becomes nonplanar, such that the bay hydrogen atoms can avoid each other. Consequently, the stabilization relative to **5** of benzenoids **10** and **12** with two adjacent kinks is less pronounced, that is, some 7−8 kcal/mol (see Table 2).

Finally, the doubly kinked structures are again stabilized (not destabilized) if one removes hydrogen atoms that are in close mutual contact. Thus, compared to the relative stability of **8**, the 1,3-[**8**−2H] biradical, in which both hydrogen atoms of one bay have been removed, gains again 1 kcal/mol in stability relative to its corresponding linear species 1,3-[**5**−2H] (see Table 2). The gain in stability relative to the linear structure is even larger, namely, 3 kcal/mol, if we remove the two central hydrogen atoms as is done in the 3,4-[**8**−2H] biradical (see Table 2). This is consistent with the fact that in the latter, that is, in 3,4-[**8**−2H], two destabilizing H−H contacts have been interrupted, one in each of the two bays of **8**, while in 1,3-[**8**−2H] only one H−H contact is (fully) removed.

Even more pronounced effects are found if the sterically nearly coinciding bay hydrogens in the highly strained and deformed benzenoids **10** and **12** are taken away. The effect is a significant gain of 5 kcal/mol in relative stability. Thus, whereas **10** and **12** are only some 7−8 kcal/mol more stable than the linear **5**, the biradicals 2,5-[**10**−2H] and 1,4-[**12**−2H] are some 12−13 kcal/mol more stable than the corresponding 2,5-[**5**−2H] and 1,4-[**5**−2H]. The additional stability of 2,5-[**10**−2H] and 1,4-[**12**−2H] goes with a pronounced geometrical relaxation which leads to completely planar structures.

3.4. Why AIM Diagnoses Bonding in the Case of Destabilization. Finally, our results once more[19−21,23−25] falsify one of the core concepts of the theory of atoms-in-molecules (AIM), namely, that the presence of bond paths and the presence of bond critical points are sufficient indicators for a stabilizing interaction. Indeed, bond paths and bond critical points exist between the bay hydrogen atoms in phenanthrene (**2**) and also in the larger hexacyclic benzenoids **5**−**14**, despite the fact that they destabilize the system. Instead, our results confirm that these AIM parameters merely diagnose the proximity or contact between charge distributions, be this contact stabilizing or destabilizing.

We have recently also pointed out that the atomic energy defined in AIM will often be stabilizing in situations where the volume of the atomic basin is reduced because of steric contact.[23,24] Here, we carry out a numerical experiment that shows explicitly that steric, destabilizing contact leads to a stabilization of the AIM atomic energy and thus to the AIM diagnosis of a bond when there is actually destabilization. To this end, we let two benzene molecules approach pointing toward each other with their C−H bonds in a D_{2h} symmetric arrangement, as shown in **14**:

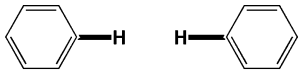

14

Not unexpectedly, the BLYP/6-311G(df,pd) energy of **14** begins to rise as soon as the two benzene molecules come into steric contact. At 2.0 (the H4−H5 separation in **2**), 1.5 and 1.0 Å, the energy of **14** is 0.7, 4.2 and 25.0 kcal/mol relative to two benzene molecules at infinite separation. Yet, the combined AIM atomic stabilization energies of the two sterically close hydrogen atoms suggest a bonding of −6.5, −17.5, and −56.5 kcal/mol when going from benzene to 2.0, to 1.5, and to 1.0 Å, respectively. Qualitatively identical results have been obtained at the BLYP/6-31G(d,p) and B3LYP/6-31G(d,p) levels of theory.

We anticipate the counter argument that **14** is not an equilibrium structure and thus the AIM concepts cannot be applied in the usual manner. However, such an argument would not be cogent. One can apply a counterforce that hinders two C−H bonds to separate and, in this way, turn this geometrical configuration into a stationary point or an equilibrium structure, despite the intrinsic H−H repulsion. A nice example of such a stationary point is provided by planar biphenyl in which the C−C bond between the phenyl moieties forces opposing *ortho*-hydrogen atoms together.[23] The computations and analyses show how the C−C bond elongates and how the opposing $C^{ortho}-H^{ortho}$ bonds bend away from each other as biphenyl is brought from its twisted equilibrium conformation to the planar conformation, which for any given C−C distance yields the strongest $H^{ortho}-H^{ortho}$ repulsion. Other examples are phenanthrene (**1**) and the kinked hexacyclic benzenoids (**6**−**13**) of the present study.

Apparently, any situation of steric congestion (or steric repulsion or steric destabilization) without[23,24] significant charge transfer from the congested atoms to the rest of the molecule would, according to the above AIM definitions, lead to a stabilization of the atomic energies and thus to the qualification of the interaction between the atoms involved as "bonding". We feel that such a qualification and therefore the physical status of some AIM theory concepts is questionable.

4. Conclusions

Phenanthrene (**2**) is more stable than anthracene (**1**) because of more stabilizing interactions in the π-electron system, as follows from our MO electronic structure analyses and quantitative bond energy decomposition in the framework of Kohn−

Sham MO density functional theory. This can be straightforwardly understood by considering the electronic structure of the two 2-methtriyl-phenyl fragments (**A**) that constitute **1** as well as **2**. The SOMO in the π system in **A** is the classical nonbonding molecular orbital (NBMO) of an uneven alternating hydrocarbon which has its largest amplitude on the external carbon atom (cf. Hückel theory of benzyl). The π SOMOs of two fragments **A** + **A** form the most stabilizing π-electron-pair bond if they are arranged such that their large π amplitudes can mutually overlap, that is, in phenanthrene.

Our analyses falsify the hypothesis of MHTB[11] on the basis of atoms-in-molecules (AIM) analyses that phenanthrene is more stable because of H−H bonding between bay hydrogen atoms. The latter H−H contact is destabilizing rather than bonding. The bond energy decomposition reveals instead increased Pauli repulsion in phenanthrene as compared to anthracene. Numerical experiments that are independent of any electronic structure model confirm that removing two (bay) hydrogens from **1** and **2** further increases the relative stability of the resulting biradical derived from phenanthrene. This is shown to hold also for larger, hexacyclic benzenoids.

Thus, we confirm the classical picture of better π bonding causing phenanthrene's enhanced stability, despite the unfavorable H−H repulsion (not H−H bonding) between bay hydrogens in phenanthrene.

Furthermore, our results once more[19−21,23−25] falsify one of the core concepts of the theory of atoms-in-molecules (AIM), namely, that the presence of bond paths and the presence of bond critical points (they exist indeed between the two bay H atoms in phenanthrene) are sufficient indicators for a stabilizing interaction. Instead, our results confirm that these AIM parameters merely diagnose the proximity or contact between charge distributions, be this contact stabilizing or destabilizing.

Acknowledgment. We thank the European Union for a Marie Curie fellowship for J. P. We also thank the Netherlands organization for Scientific Research (NWO−CW), the Spanish Ministerio de Educación y Ciencia (Project CTQ2005-08797-C02-01), the Catalan Departament d'Universitats Recerca i Societat de la Informació (Project 2005SGR-00238), and the European Union (HPC program) for financial support. Excellent service by the Stichting Academisch Rekencentrum Amsterdam (SARA) and the Centre de Supercomputació de Catalunya (CESCA) is gratefully acknowledged.

Supporting Information Available: Cartesian coordinates for all species occurring in this work. This material is available free of charge via the Internet at http://pubs.acs.org.

JO061637P